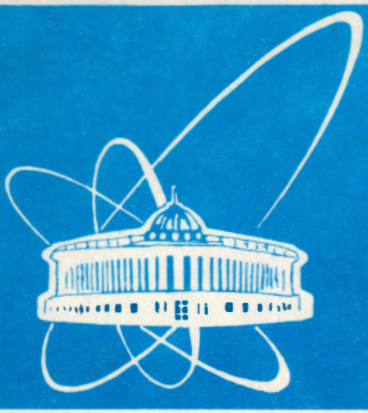

объединенный
институт
ядерных
исследований
дубна

E17-94-59

N.M.Plakida, V.S.Oudovenko, V.Yu.Yushankhai

TEMPERATURE AND DOPING DEPENDENCE OF QUASIPARTICLE SPECTRUM FOR HOLES IN SPIN-POLARON MODEL OF COPPER OXIDES

Submitted to «Physical Review B»

1994

1 Introduction

The problem of a hole motion in an antiferromagnetic (AF) background have attracted much attention last years. That is mainly due to a hope to elucidate the nature of the carriers involved in the high-T_c superconductivity in copper oxides. It is believed that the essential features of the problem are described by the $t-J$ model with Hamiltonian written as

$$H_{t-J} = t \sum_{\langle ij \rangle \sigma} \tilde{c}^{+}_{i\sigma} \tilde{c}_{j\sigma} + J \sum_{\langle ij \rangle} \mathbf{S}_i \mathbf{S}_j = H_t + H_J. \qquad (1)$$

Here $< ij >$ indicates nearest-neighbor pairs, $\tilde{c}^{+}_{i\sigma} = c^{+}_{i\sigma}(1 - n_{i,-\sigma})$ are the electron operators with the constraint of no double occupancy. At the half-filling limit only the Heisenberg part of the Hamiltonian (1) is relevant and it describes an AF insulating state. A hole doped in this state propagates on the lattice strongly interacting with a spin background. The properties of a single hole doped in the Néel spin background have been analyzed intensively with various numerical and analytical methods. Among them are the exact diagonalization of small clusters [1] and variational calculations [2]. A rather transparent description within a "string" picture have been developed by several authors [3]. A perturbative approach to the problem was proposed by Schmitt – Rink, Varma and Ruckenstein [4] and developed further by Kane, Lee and Read [5] and Martinez and Horsch [6]. In this approach a slave fermion representation for the $t-J$ model was used and a hole propagation was treated within the self-consistent Born approximation (SCBA). In this formulation of the $t-J$ model a hole motion, which is only possible due to its strong coupling to spin-wave excitations, is regarded as a sort of spin polaron propagation [6], [7]. The results obtained in this approach turned out to be in a good agreement with those for exact diagonalization of small clusters [1], [6] for a wide range of a parameter value J/t.

Now there exists a consensus that a hole doped in a quantum Néel background can propagate coherently with the quasiparticle (QP) band width of order of the exchange constant J and with a hole ground-state energy minima at momenta $\mathbf{k} = (\pm\pi/2, \pm\pi/2)$. The calculated spectral density function [1], [5], [6] reveals a QP peak of intensity $Z_k \approx J/t$ at low energy side of the spectrum and this peak is well separated from the broad incoherent part which has a width of about $6 \div 7t$.

Being so successful in reproducing the single-hole results calculated by exact diagonalization method the perturbative approach within the SCBA is expected to provide a reasonable scheme for examining quasiparticle hole properties at finite doping as well. Some progress along this way has been gained by Igarashi and Fulde [8]. By developing a standard diagrammatic technique at $T = 0$ they found that at finite doping a hole Green's function changes in a rather complicated way and new incoherent states below the QP peaks appear. Nevertheless, as it was argued in [8] to the first order in δ the QP band characteristics change negligibly as compared to the single-hole results [8]. Therefore, the quasiholes being treated as noninteracting ones, fill up four "hole pockets" around the degenerate minima at the momenta $\mathbf{k} = (\pm\pi/2, \pm\pi/2)$. Some arguments have also been given in [8] that the fraction of the Brillouin zone covered by these pockets is equal to hole concentration δ.

Below we present the results of calculations of hole's spectral properties based on the same formulation of the $t - J$ model as in [5] – [8]. We assume a quantum Néel state for magnetic background and develop further the self-consistent Born approximation to calculate with more accuracy the spectral density function $A(k, \omega)$ and the momentum distribution function $N(k)$ for holes at finite doping and finite temperatures. To this end the irreducible

Green's function method will be used to derive the two-time hole Green's function. As compared to the single-hole case [5], [6] now the self-energy involves both the processes of emitting and absorbing of spin waves and, that is more, incorporates temperature dependent corrections. The integral equation for the self-energy is solved numerically on the 16 $\times$ 16 lattice with good accuracy that allows us to compute $A(k, \omega)$ and $N(k)$ and analyze a quasihole behaviour at various concentrations δ and temperatures T. While performing the computations we do not use from the beginning any additional ansatz about the shape of $A(k, \omega)$ that differs our approach from that of presented in [8].

In this paper we are not interested in effects of renormalization of spin-wave excitations due to their coupling to holes and treat spin waves as bare ones. Instead, focusing on the doping and temperature dependence of hole's spectral properties we examine not only the low concentration limit, but extend our calculations to a regime of moderate hole concentration, $\delta \geq 10\%$, as well. A validity of such an extension will be discussed below.

In Sec. II we describe the effective Hamiltonian in a slave-fermion Schwinger boson representation. The Dyson's equation for a hole two-time Green's function is derived and the self-energy is obtained in a SCBA. An iteration procedure to solve an integral equation for the self-energy is discussed shortly in Sec. III and numerical results are presented and analyzed. Section 4 contains the concluding remarks.

2 Effective Hamiltonian and Green's function for holes

We make use of a slave-fermion Schwinger boson factorization for electron operators $\tilde{c}_{i\sigma} = h_i^+ b_{i\sigma}$, where the slave-fermion operator h_i^+ generates a hole at site i and the boson operator $b_{i\sigma}$ keeps track of the spins. Using this factorization the $t-J$ model (1) can be mapped onto a new effective Hamiltonian in a few steps.

We consider a quantum Néel state and divide the square lattice into $A(\uparrow)$ and $B(\downarrow)$ sublattices. Fist to simplify a matter let us perform a 180° rotation of the spins at the B sublattice that is equivalent to the replacement

$$\tilde{c}_{i\sigma} \to \tilde{c}_{i,-\sigma}, \quad S_i^{\pm} \to S_i^{\mp}, \quad S_i^z \to -S_i^z \qquad i \in B. \tag{2}$$

Then the Néel state can be considered as a condensate of $b_{i\uparrow}$ bose field and, hence, to the lowest order in $1/S$ expansion $b_{i\uparrow} = \sqrt{2S}$. The uncondensed bosons $b_{i\downarrow}$ turn into spin-excitation operators that can be written after Bogolubov $u-v$ transformation as follows

$$b_{q\downarrow} = u_q \alpha_q + v_q \alpha_{-q}^+, \tag{3}$$

where $b_{q\downarrow}$ is the Fourier transform of $b_{i\downarrow}$ operators in the first Brillouin zone and

$$u_q = \left[\frac{1+\sqrt{1-\gamma_q^2}}{2\sqrt{1-\gamma_q^2}}\right]^{1/2} \qquad v_q = -\mathrm{sign}(\gamma_q)\left[\frac{1-\sqrt{1-\gamma_q^2}}{2\sqrt{1-\gamma_q^2}}\right]^{1/2}, \tag{4}$$

$$\gamma_q = \frac{1}{2}(\cos q_x + \cos q_y) \tag{5}$$

Here the lattice spacing is taken as unity. Finally, we arrive at

$$H_t = \sum_{kq} h_k^+ h_{k-q}[M_1(k,q)\alpha_q + M_2(k,q)\alpha_{-q}^+] - \mu \sum_k h_k^+ h_k, \tag{6}$$

$$H_J = \sum_q \omega_q \alpha_q^+ \alpha_q, \qquad \omega_q = SzJ(1-\delta)^2\sqrt{1-\gamma_q^2} \tag{7}$$

where $\delta = \langle h_i^+ h_i \rangle$ is a hole concentration, $z = 4$ and

$$M_1(k,q) = zt\sqrt{\frac{2S}{N}}(u_q\gamma_{k-q} + v_q\gamma_k), \tag{8}$$

$$M_2(k,q) = zt\sqrt{\frac{2S}{N}}(u_q\gamma_k + v_q\gamma_{k-q}), \tag{9}$$

With more details the effective Hamiltonian (6) – (9) is derived in a number of papers [5], [6], [8]. To distinguish this Hamiltonian from the original $t-J$ model we call it as the magnetic polaron model. It is worth noting also that an additional term proportional to a chemical potential μ is involved explicitly in (6). A variation of μ, as a function of hole concentration δ and temperature T, should be calculated self-consistently.

Let us now define a single-particle two-time retarded Green's function

$$\langle\langle h_k(t)|h_k^+(t')\rangle\rangle = -i\theta(t-t')\langle\{h_k(t), h_k^+(t')\}\rangle, \tag{10}$$

where $\theta(t)$ is the step function and $\{,\}$ stands for the anticommutator. The Fourier transform is defined by

$$\langle\langle h_k|h_k^+\rangle\rangle_\omega = \int_{-\infty}^{+\infty} dt e^{i\omega(t-t')}\langle\langle h_k(t)|h_k^+(t')\rangle\rangle \equiv G(k,\omega)\,. \tag{11}$$

To obtain an equation of motion for the Green's function one may follow Ref. [9] differentiating with respect to both times t and t'. Then after the Fourier transform we have a set of two equations

$$(\omega+\mu)G(k,\omega) = 1 + \sum_q \langle\langle h_{k-q}B(k,q)|h_k^+\rangle\rangle_\omega\,, \tag{12}$$

$$(\omega+\mu)\langle\langle h_{k-q}B(k,q)|h_k^+\rangle\rangle_\omega = \sum_{q'}\langle\langle h_{k-q}B(k,q)|h_{k-q'}^+B^+(k,q')\rangle\rangle_\omega\,, \qquad (13)$$

where

$$B(k,q) = M_1(k,q)\alpha_q + M_2(k,q)\alpha_{-q}^+. \qquad (14)$$

Substituting (13) into (12) and defining the zero order Green's function $G_0^{-1}(k,\omega) = \omega+\mu$, we get the equation

$$G(k,\omega) = G_0(k,\omega) + G_0(k,\omega)T(k,\omega)G_0(k,\omega) \qquad (15)$$

where the scattering matrix $T(k,\omega)$ is a higher order Green's function

$$T(k,\omega) = \sum_{qq'}\langle\langle h_{k-q}B(k,q)|h_{k-q'}^+B^+(k,q')\rangle\rangle_\omega. \qquad (16)$$

The Eq.(15) can be also rewritten as the Dyson's equation

$$G^{-1}(k,\omega) = G_0^{-1}(k,\omega) - \Sigma(k,\omega), \qquad (17)$$

where the self-energy $\Sigma(k,\omega)$ is connected with the scattering matrix by the equation $T = \Sigma + \Sigma G_0 T$. Hence, one can see that the self-energy $\Sigma(k,\omega)$ is the irreducible part of $T(k,\omega)$:

$$\Sigma(k,\omega) = T^{(irr)}(k,\omega), \qquad (18)$$

which can be evaluated by a proper decoupling procedure for correlation functions entering in (16) as follows

$$\langle h_{k-q'}^+B^+(k,q')h_{k-q}(t)B(k,q,t)\rangle \simeq \langle h_{k-q}^+h_{k-q}(t)\rangle\langle B^+(k,q)B(k,q,t)\rangle\delta_{qq'} \simeq$$

$$\simeq \delta_{qq'}\langle h_{k-q}^+h_{k-q}(t)\rangle\{M_1^2(k,q)\langle\alpha_q^+\alpha_q(t)\rangle + M_2^2(k,q)\langle\alpha_{-q}\alpha_{-q}^+(t)\rangle\}\,. \qquad (19)$$

Using the spectral representation for Green's functions we obtain the following intermediate result for the self-energy

$$\Sigma(k,\omega) = \sum_q \int_{-\infty}^{+\infty}\frac{d\omega_1}{\pi}\int_{-\infty}^{+\infty}\frac{d\omega_2}{\pi}\frac{e^{\beta(\omega_1+\omega_2)}+1}{(e^{\beta\omega_1}+1)(e^{\beta\omega_2}-1)}\frac{\mathrm{Im}\langle\langle h_{k-q}|h_{k-q}^+\rangle\rangle_{\omega_1+i\eta}}{\omega-(\omega_1+\omega_2)+i\eta}\times$$

$$\{M_1^2(k,q)\mathrm{Im}\langle\langle\alpha_q|\alpha_q^+\rangle\rangle_{\omega_2+i\eta} + M_2^2(k,q)\mathrm{Im}\langle\langle\alpha_{-q}^+|\alpha_{-q}\rangle\rangle_{\omega_2+i\eta}\}\,. \qquad (20)$$

Further we neglect self-energy corrections to the spin-wave Green's function that results in the simplest form for the spectral density function

$$-\tfrac{1}{\pi}\mathrm{Im}\langle\langle\alpha_q|\alpha_q^+\rangle\rangle_\omega = \delta(\omega-\omega_q), \qquad (21)$$

$$-\tfrac{1}{\pi}\mathrm{Im}\langle\langle\alpha_{-q}^+|\alpha_{-q}\rangle\rangle_\omega = -\delta(\omega+\omega_q).$$

Finally, we obtain

$$\Sigma(k,\omega) = \Sigma_1(k,\omega) + \Sigma_2(k,\omega) \qquad (22)$$

$$\Sigma_1(k,\omega) = \sum_q M_1^2(k,q)\int_{-\infty}^{+\infty}d\varepsilon\frac{A(k-q,\varepsilon)}{\omega-\varepsilon-\omega_q+i\eta}[1-n(\varepsilon)+N(\omega_q)], \qquad (23)$$

$$\Sigma_2(k,\omega) = \sum_q M_2^2(k,q)\int_{-\infty}^{+\infty}d\varepsilon\frac{A(k-q,\varepsilon)}{\omega-\varepsilon+\omega_q+i\eta}[n(\varepsilon)+N(\omega_q)], \qquad (24)$$

where $n(\varepsilon) = (e^{\beta\varepsilon}+1)^{-1}$ and $N(\omega) = (e^{\beta\omega}-1)^{-1}$ and

$$A(k,\omega) = -\frac{1}{\pi}\mathrm{Im}G(k,\varepsilon+i\eta), \qquad (25)$$

is the spectral density for holes. To make a set of equations (17) and (20) – (25) self-consistent the following equation for the chemical potential μ should be adopted

$$\delta = \frac{1}{N}\sum_k\int_{-\infty}^{+\infty}d\varepsilon n(\varepsilon)A(k,\varepsilon). \qquad (26)$$

As it is shown in Appendix the set of equation we derived is equivalent at $T = 0$ to that obtained in standard diagrammatic technique within SCBA. However, in our formulation a temperature dependence is taken into account in explicit way.

3 Numerical solution and discussions

In this section we present the numerical results for the set of self-consistent equations (17), (22) – (26). We consider two dimentional square lattice on the 16×16 cluster exploiting all possible symmetries. For instance, one may deal only with 25 point in the irreducible wedge of the antiferromagnetic Brillouin zone (AF BZ). The frequency space is divided into meshes with their size $0.005t$ to provide sufficient energy resolution. To make the iteration procedure convergent a small imaginary part $\eta = 0.01t$ to the frequency in the Green's function is added. The numerical procedure was organized in such way that at given δ and T a value for the chemical potential μ and the spectral density function $A(k,\omega)$ were calculated self-consistently by iteration procedure. Typically, after 40-50 iterations the chemical potential converged to some fixed value $\mu = \mu(\delta, T)$ and the sum rule on $A(k,\omega)$ was fulfilled with accuracy better than 1%. Below presented $A(k,\omega)$ at given δ and T we measure frequency from the chemical potential $\mu(\delta, T)$. By performing calculations with $J = 0.4$ and $J = 0.2$ (from now we will refer all quantities in unit of t) we found no qualitative differences. Therefore the data with $J = 0.4$ will be only discussed.

3.1 Spectral density $A(k,\omega)$

We started calculating the spectral density function $A(k,\omega)$ for the single hole at $T = 0$ and found substantial agreement with numerical results presented in Ref. [6]. Further referring these results we discuss how the hole

spectral properties will be changed with increasing hole concentration δ and temperature T.

In Fig. 1 we show spectral function for several $\mathbf{k}$-points calculated at $T = 0$ and $\delta = 3\%$. Let us first discuss the $\mathbf{k}$-points belonging to the edge of the AF BZ, Fig. 1(a) and (b). There are no any visible changes in the shape of $A(k,\omega)$ as compared to the single-hole case, $\delta \to 0$. More precisely, calculations give a few percentage increase of a QP spectral weight $Z(\mathbf{k})$ (the integrated area under a QP peak). For instance, the value of $Z(\frac{\pi}{2}, \frac{\pi}{2})$ increases from $Z \simeq 0.33$ at $\delta \to 0$ to $Z \simeq 0.35$ at $\delta = 3\%$ and this tendency is kept for higher δ (see Table 1). We found that the QP peak for $\mathbf{k} = (\frac{\pi}{2}, \frac{\pi}{2})$ is located below μ at $\omega_{QP}(\frac{\pi}{2}, \frac{\pi}{2}) \simeq -0.01$ while for $\mathbf{k} = (0, \pi)$ it is above μ, $\omega_{QP}(0, \pi) > 0$.

For the momenta $\mathbf{k}$ laying far from the AF BZ edge the spectral function $A(k,\omega)$ is modified with doping in another way. Actually, one can see from Figs. 1(c) and 1(d) that in comparison with the single hole case for $\mathbf{k} = (0, \frac{\pi}{2})$ and (0,0) the spectral density is redistributed so that a new incoherent broad structure, as first has been noted in Ref. [10], appears far below the chemical potential. The spectral weight for this new structure is proportional to δ.

The peculiarities in the shape of $A(k,\omega)$ mentioned above become more pronounced with further increasing of hole concentration. The spectral density $A(k,\omega)$ calculated at $T = 0$ and $\delta = 10\%$ is shown in Fig. 2 for two most representative $\mathbf{k}$-points: $\mathbf{k} = \mathbf{k}^* = (\frac{\pi}{2}, \frac{\pi}{2})$ and $\mathbf{k} = (0,0)$. Examining the data for $\mathbf{k}^*$, Fig. 2(a) and Table 1, we noticed about 10% increase of the QP spectral weight $Z(\mathbf{k}^*)$. Also the QP peak is shifted to the position $\omega_{QP}(\mathbf{k}^*) \simeq -0.055$. For $\mathbf{k} = (0,0)$, Fig. 2(b), a strong suppression of the QP peak at $\omega \simeq 0.8$ and forming a band of incoherent excitations below the chemical potential are seen.

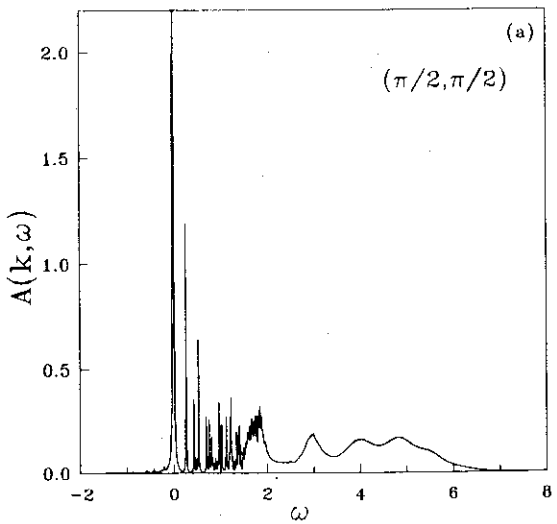

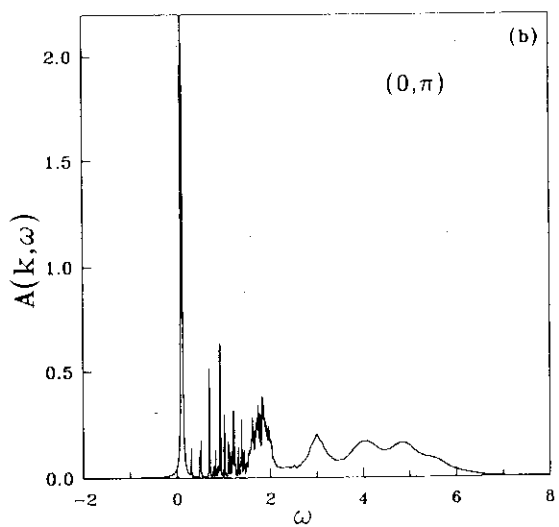

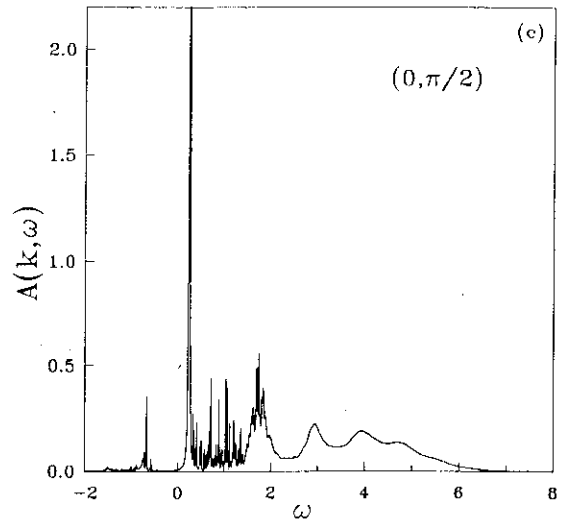

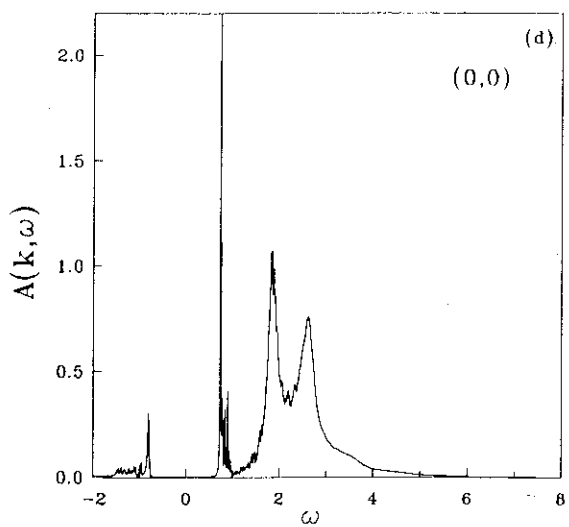

Fig. 1. Spectral functions $A(k,\omega)$ for $J = 0.4$ at $T = 0$ and hole concentration $\delta = 3\%$: $\mathbf{k} = (\pi/2,\pi/2)$ (a); $(0,\pi)$ (b); $(0,\pi/2)$ (c); $(0,0)$ (d). A frequency ω is measured from the chemical potential μ.

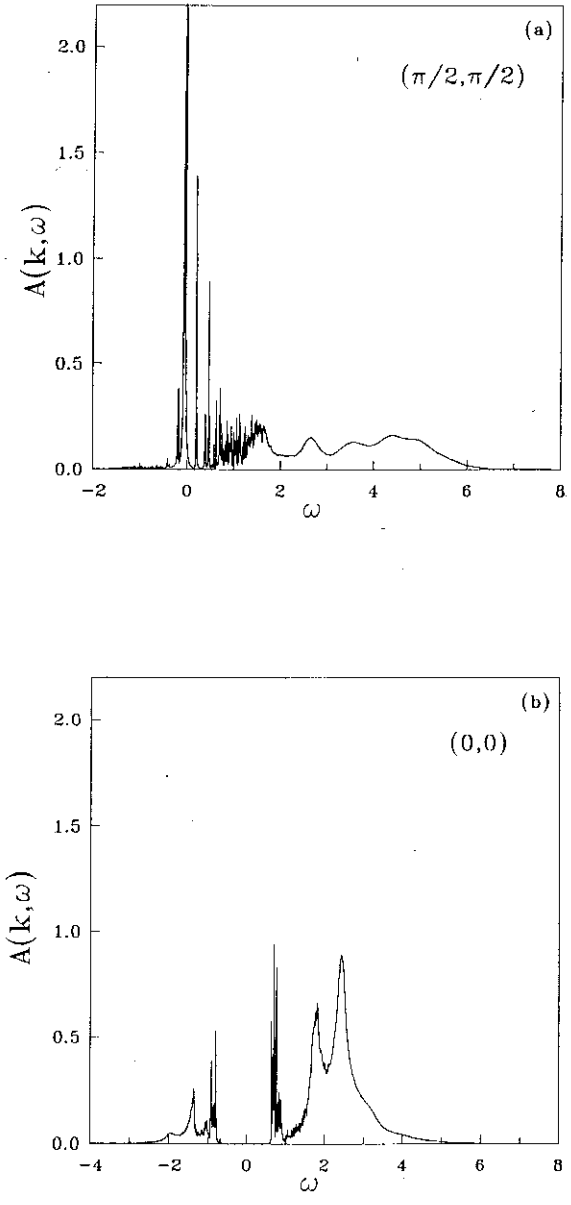

Fig. 2.Spectral functions $A(k,\omega)$ for $T = 0$ and $\delta = 10\%$ at $\mathbf{k} = (\pi/2, \pi/2)$ (a) and $\mathbf{k} = (0,0)$ (b).

The energy minimum of the QP band was found at $\mathbf{k} = \mathbf{k}^*$ throughout our computations. Figure 3 shows doping dependence of the energy $E(\mathbf{k}^*) = \omega_{QP}(\mathbf{k}) + \mu$ of the lowest QP peak and the chemical potential μ. We think that our finite-cluster computations at extremely low concentration, $\delta < \delta_1$, are not rigorous enough that results in inverse relative position of μ and $E(\mathbf{k}^*)$ i.e. $\mu < E(\mathbf{k}^*)$ in this region. Being measured from μ the position of the lowest QP peak is fitted with a good accuracy by the following dependence $E(\mathbf{k}^*) - \mu = \omega_{QP}(\mathbf{k}^*) \approx -1.5J(\delta - \delta_1)$ for $\delta > \delta_1 \approx 1.5\%$.

By analogy with a conventional case of free-fermion gas we associate the quantity $\mu - E(\mathbf{k}^*)$, taken for $\delta > \delta_1$, with the Fermi energy for a quasihole gas. We can also define a degeneracy temperature as $T_d(\delta) = 1.5J\delta$. It means that at $T > T_d(\delta)$ one should expect a different behaviour for the quasihole gas as compared to the low temperature limit $T \ll T_d$. We examine this hypothesis in Sect. 3.2 considering temperature variations for the hole-momentum distribution function $N(k)$.

Now we address the problem of the temperature dependence of quasihole spectral properties. Analyzing a variety of spectral densities $A(k,\omega)$ calculated in a wide temperature interval and several values of δ we found no significant changes in the shape of $A(k,\omega)$ up to $T \sim T_d(\delta)$. At a given δ the only temperature effect is an equal shift of $A(k,\omega)$ to higher values of ω for all $\mathbf{k}$. In particular, the lowest QP peak for $\mathbf{k}^*$ is close to zero energy, $\omega_{QP}(\mathbf{k}^*) \simeq 0$, $T \simeq T_d(\delta)$.

Such a behaviour is an effect of temperature variation of the chemical potential $\mu = \mu(\delta, T)$, (see Fig. 4), crossing the bottom of the QP band (i.e. the lowest QP peak energy) when temperature reaches the critical value $T \simeq T_d(\delta)$. With further increasing in T, as it can be seen from Fig. 5, the sharp structure

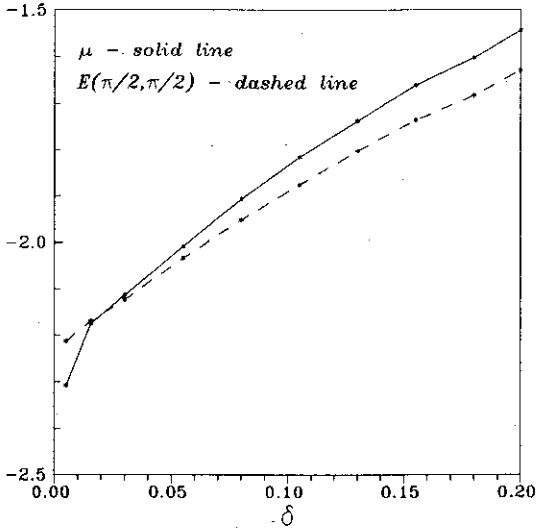

Fig. 3. Chemical potential μ (solid line) and energy of the lowest QP peak $E(\mathbf{k}^* = (\pi/2, \pi/2)) = \omega_{QP}(\mathbf{k}^*) + \mu$ vs δ at $T = 0$.

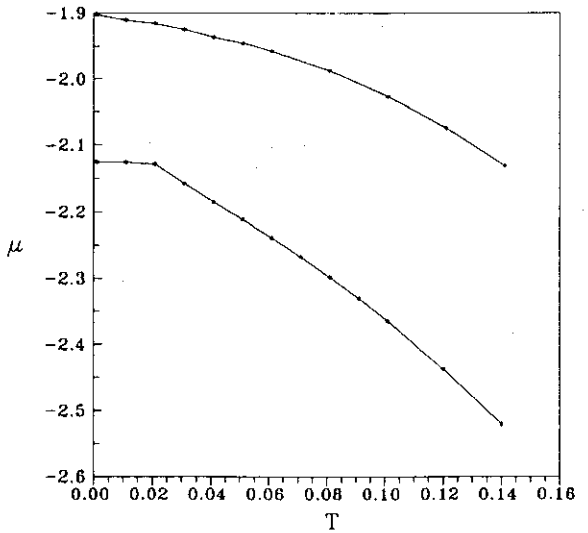

Fig. 4. Temperature dependence of μ for $\delta = 3\%$ (lower curve) and $\delta = 10\%$ (upper curve).

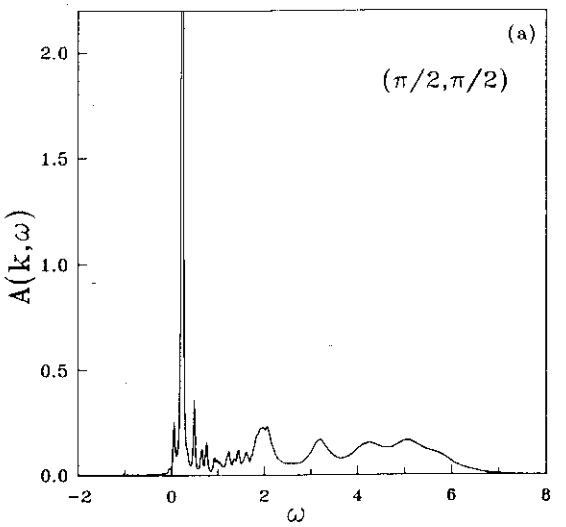

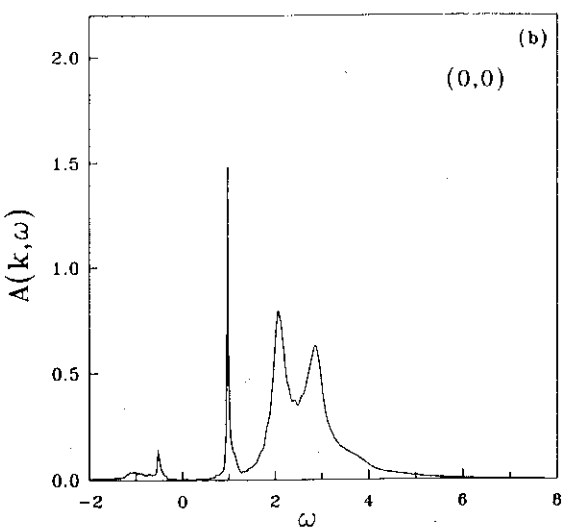

Fig. 5. Spectral functions $A(k, \omega)$ for $T = 0.1$ and $\delta = 3\%$ at $\mathbf{k} = (\pi/2, \pi/2)$ (a) and $\mathbf{k} = (0, 0)$ (b).

Table 1: QP spectral weight $Z(\mathbf{k}^*)$ and QP peak position $\omega_{QP}(\mathbf{k}^*)$ at $\mathbf{k}^* = (\pi/2, \pi/2)$ for different hole concentrations and $T = 0$. The concentration $\delta \approx 0.4\%$ corresponds to a single-hole case

δ	$Z(\mathbf{k}^*)$	$\omega_{QP}(\mathbf{k}^*)$
0.4%	0.329	0.005
3%	0.353	-0.010
10%	0.369	-0.055
20%	0.373	-0.085

Table 2: The Dependence of $Z(\mathbf{k}^*)$ and $\omega_{QP}(\mathbf{k}^*)$ on temperature
($\delta = 3\%$)

T	$Z(\mathbf{k}^*)$	$\omega_{QP}(\mathbf{k}^*)$
0.000	0.353	-0.010
0.017	0.339	0.005
0.061	0.333	0.115
0.100	0.321	0.225

of the spectral density is smeared out and all QP peaks are shifted and become above the chemical potential ($\omega_{QP}(k) > 0$).

It is worth noting a weak temperature renormalization of QP spectral weights $Z(k)$ for k-pints at the AF BZ edge as can be seen for $\delta = 3\%$ and different temperatures from Table 2.

To get more insight into the problem we compare the data for the spectral density $A(k,\omega)$ and the imaginary part of the self-energy $\Gamma(k,\omega) = -\mathrm{Im}\Sigma(k,\omega)$. Figures 6(a) and (b) show $\Gamma(\mathbf{k}^*,\omega)$ obtained for $\delta = 10\%$ at $T = 0$ and $T = 0.1$, respectively. Calculations at low concentration, e.g. $\delta = 3\%$, give similar results.

Figure 6(a) shows that $\Gamma(\mathbf{k}^*,\omega) \approx 0$ (we found $\Gamma \leq 10^{-14}$) in the frequency interval $|\omega| \leq 0.2$ where the QP peak is located. This clearly indicates that there are no low-energy states to which the quasihole can scatter and therefore it has infinite lifetime. For higher frequencies, $0.2 < \omega \leq 7$, $\Gamma(k,\omega)$ grows sharply giving a wide distribution with a large characteristic amplitude. Since in this region $|\omega - \mathrm{Re}\Sigma(k,\omega)| \ll \Gamma(k,\omega)$ we can write

$$A^{(incoh)}(\mathbf{k}^*,\omega) \simeq \frac{1}{\pi\Gamma(\mathbf{k}^*,\omega)}. \qquad (27)$$

Comparing $\Gamma(\mathbf{k}^*,\omega)$ calculated at higher temperature $T = 0.1$, Fig. 6(b), with corresponding $A^{(incoh)}(\mathbf{k}^*,\omega)$, we conclude that the same relation (27) between them is hold. Though QP width $\Gamma_{\mathbf{k}^*} = \Gamma(\mathbf{k}^*,\omega = \omega_{QP})$ increases strongly with temperature and reaches the value $\Gamma \sim 0.01$ at $T = 0.1$, nevertheless, it remains still negligibly small. We come to the same conclusion with respect to other k-points arranged along the AF BZ edge, Fig. 7.

Thus we can infer that quasihole states remain a well-defined excitations being stable over a wide range of temperature and hole concentration.

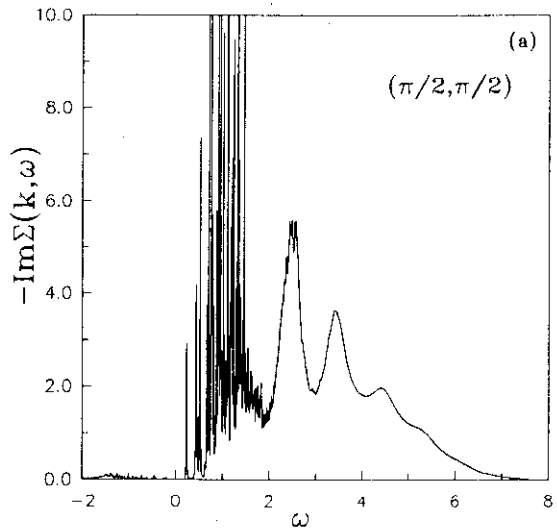

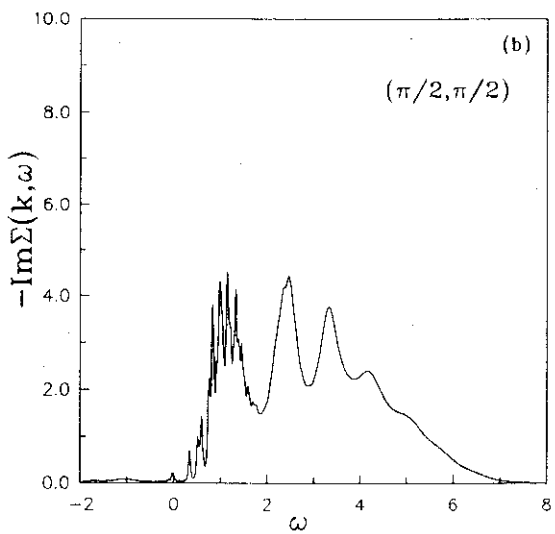

Fig. 6. Imaginary parts of the self-energy operator $\Sigma(k,\omega)$ for $\delta = 3\%$ at $\mathbf{k} = (\pi/2,\pi/2)$: $T = 0$ (a); 0.1 (b).

Presented numerical results for the spectral density could be fitted with some accuracy by the following formula:

$$A(k,\omega) \simeq \frac{Z_k}{\pi} \frac{\gamma_k}{(\omega - \omega_{QP}(k))^2 + \gamma_k^2}\Big|_{\omega \simeq \omega_{QP}(k)} + \frac{1}{\pi\Gamma(k,\omega)}\Big|_{\omega \neq \omega_{QP}(k)} =$$

$$= A^{(coh)}(k,\omega) + A^{(incoh)}(k,\omega) \qquad (28)$$

where $\gamma_k = Z_k\eta$ and $\eta = 0.01$. The broadening of the coherent peak seen in our figures for $A(k,\omega)$ is an artifact due to finite η introduced in our numerical procedure to facilitate computations.

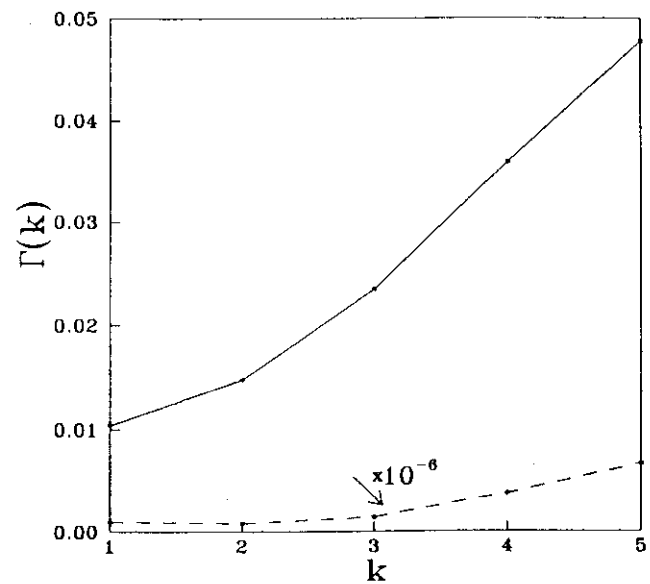

Fig. 7. QP width $\Gamma(k,\omega = \omega_{QP})$ dependence for $T = 0.1$ (solid line) and $T = 0.01$ (dashed line multiplied by 10^{-6}) at five k-points: 1 – (0,0); 2 – $(\frac{\pi}{8},\frac{7\pi}{8})$; 3 – $(\frac{\pi}{4},\frac{3\pi}{4})$; 4 – $(\frac{3\pi}{8},\frac{5\pi}{8})$; 5 – $(\frac{\pi}{2},\frac{\pi}{2})$.

3.2 Momentum distribution $N(k)$

In this subsection we present data for the hole-momentum distribution function $N(k)$ defined as

$$N(k) = \int_{-\infty}^{+\infty} d\omega \;\; n(\omega) A(k,\omega) \tag{29}$$

First we calculate $N(k)$ at $T = 0$ for several hole concentrations, Figs. 8 – 10. One can see four quasiparticle "pockets" at $\mathbf{k} = (\pm\frac{\pi}{2}, \pm\frac{\pi}{2})$ superimposed over the smooth slightly **k**-dependent background. Let us first discuss an origin for a partial, of order δ, occupancy for k-points far from the edge of AF BZ. To this end one should take into account a particular shape for the spectral density $A(k,\omega)$ at these points, as seen from Figs. 1(c), (d) and 2(b). It is clear that while calculating $N(k)$ according to (29) the high-energy part of the spectral density is cut off by the Fermi factor and only the low-energy incoherent part $A^{(incoh)}(k, \omega < 0)$ contributes to background:

$$N(k) = \int_{-\infty}^{0} d\omega \; A^{(incoh)}(k,\omega) = N_B(k). \tag{30}$$

As found numerically, the spectral weight for the low-energy incoherent part $A^{(incoh)}(k, \omega < 0)$ is approximately equal to δ. Hence, it is possible to estimate the background value as $N_B(k) \simeq \delta$.

Now we can consider **k**-points at the vicinity of AF BZ edge. As was pointed out above there is no incoherent part of the spectral density below the chemical potential, i.e. $A^{(incoh)}(k, \omega < 0) \equiv 0$ for this region of BZ. At $T = 0$ QP sates for k-points near $\mathbf{k}^*$ are located below μ and $\omega_{QP}(k) < 0$. Just this states lead to appearance of QP "pockets". It is easy to get from (29) using formula (28) for $A(k,\omega)$ that at zero temperature the occupancy is equal to $N(k) \simeq Z_k = N_{QP}(k)$ inside the "pocket" and $N_{QP}(k) = 0$ outside.

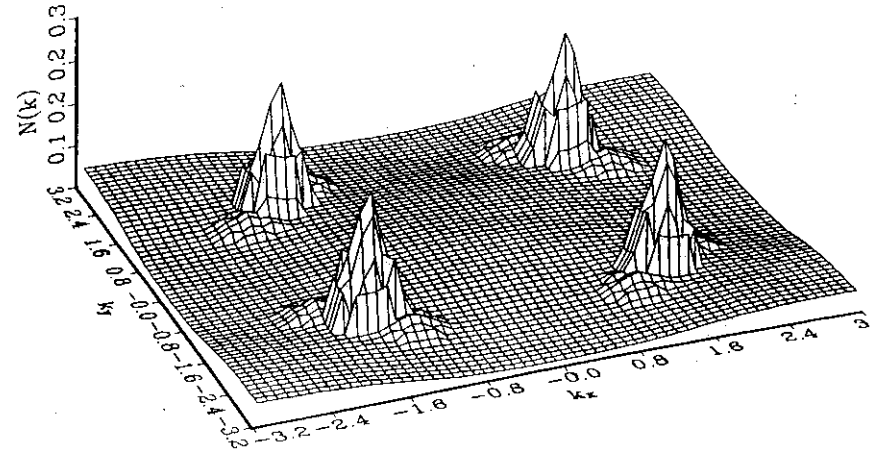

Fig. 8.Hole-momentum distribution function $N(k)$ for $\delta = 3\%$ at $T = 0$. Four quasiparticle hole "pockets" at $\mathbf{k} = (\pm\frac{\pi}{2}, \frac{\pi}{2})$ are clearly see on smoothly **k**-dependent background.

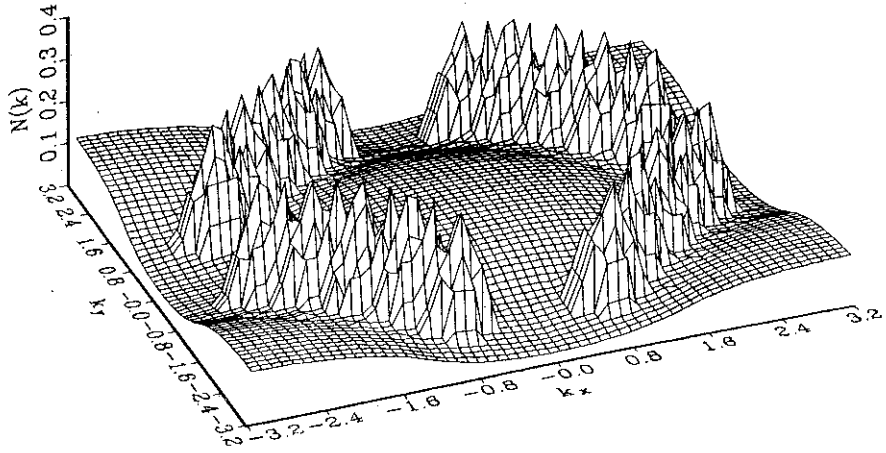

Fig. 9.Hole-momentum distribution function $N(k)$ for $\delta = 10\%$ at $T = 0$.

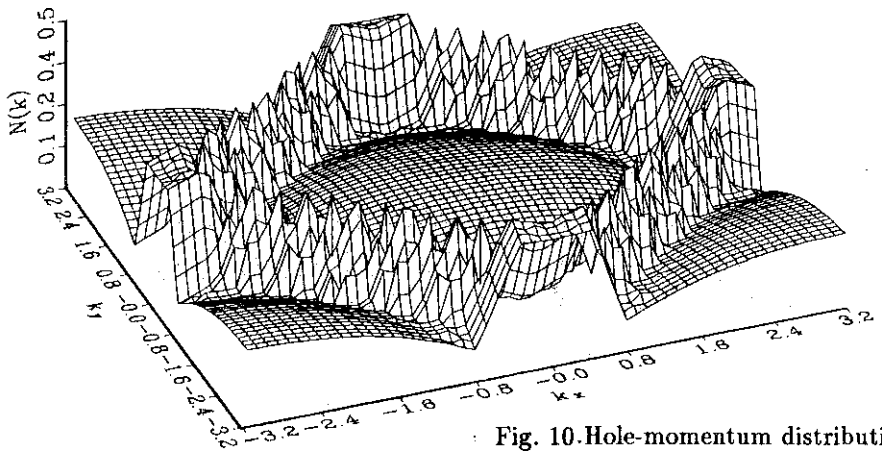

Fig. 10.Hole-momentum distribution function $N(k)$ for $\delta = 20\%$ at $T = 0$.

The volume covered by "pockets" in the k-space increases with δ. However, we cannot obtain sharp Fermi surface at $T = 0$ due to our artificial broadening of $A(k,\omega)$ spectra of order $\eta = 0.01$

Studying temperature effects at a given concentration δ we find that the momentum distribution function $N(k)$ changes dramatically when temperature reaches the value $T \sim T_d(\delta)$. Momentum distribution calculated for $\delta = 3\%$ at temperature somewhat higher than $T_d(3\%) \simeq 0.01$ is shown in Fig. 11 (pay attention on the change of scale). "Four-pocket" structure for $N(k)$, which exists at $T \ll T_d$, almost washed out at $T \geq T_d$. This peculiarity can be easily understood if one takes into account a temperature shift of the QP spectrum $\omega_{QP}(k)$. As discussed in the previous section, for $T > T_d(\delta)$ all the QP peaks occur above the chemical potential and, hence, $\omega_{QP}(k) > 0$. Thus the Fermi-factor leads to a strong reduction of the occupancy weight in comparison with the low-temperature value $Z(k)$ that explains a disappearance of the quasihole "pockets". We also found that background value $N_B(k)$ is almost T-independent and $N_B(k) \approx \delta$.

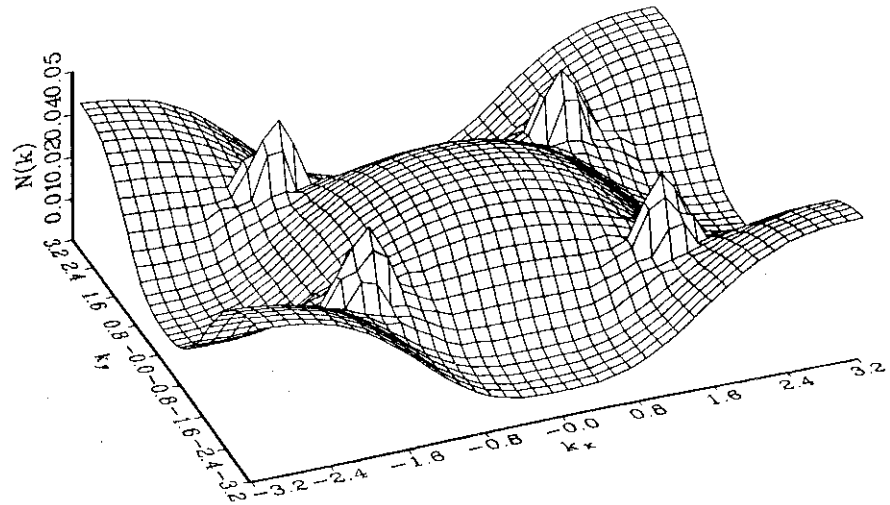

Fig. 11.Hole-momentum distribution function $N(k)$ for $\delta = 3\%$ at $T \simeq 0.017 > T_d$. Pay attention on the change of scale.

4 Conclusion

Based on the t-J model we have studied a doped antiferromagnet and calculated the spectrum of hole excitations in a wide rage of temperature, $T \leq 0.1$, and hole concentration, $\delta \leq 0.2$. The t-J model was treated in a slave-fermion representation with holes considered as spinless fermions strongly coupled to spin excitations in a quantum Néel background. The effect of strong hole-spin coupling is very important in forming the hole spectrum since there is no bare kinetic term in the effective Hamiltonian we consider. Similar to other approaches [4], [5], [6], [8] the problem was investigated within the self-consistent Born approximation based on the two-time Greens function formalism for finite temperatures. Mainly we were interested in the stability of QP hole excitation in respect of hole doping and temperature variation.

For this purpose we have calculated the hole spectral density function $A(k,\omega)$ Eq. (25) and the imaginary part of the hole self-energy $\Gamma(k,\omega)$ whose temperature and doping dependence have been studied. For **k**-points positioned at the AF BZ edge $\mathbf{k} = (\pi/2,\pi/2), (0,\pi)$, the spectral density $A(k,\omega)$ clearly shows a quasiparticle peak, with intensity $Z(k) \sim J$, at $\omega = \omega_{QP}(k)$ (see Figs. 1(a),(b), 2(a) and 5(a)) which is stable in a wide range of T and δ (see Figs. 5, 6, 7). A broad band of incoherent states with spectral weight $(1 - Z(k))$ at $\omega > \omega_{QP}(k)$ is also seen.

For low temperatures, $T \leq T_d(\delta) \simeq 1.5J\delta$, the QP peak at $\mathbf{k} = \mathbf{k}^* = (\pi/2,\pi/2)$ is positioned below the chemical potential, $\omega_{QP} = E(\mathbf{k}) - \mu < 0$ (Fig. 3) that results in "four-pockets" shape for the momentum distribution function $N(k)$ (Fig. 8 – 10). But at $T > T_d(\delta)$ this picture is completely washed out (Fig. 11).

Since the intrinsic widths Γ_k for QP states remain negligibly small at $T \geq T_d(\delta)$ a disappearance of the "pockets" in $N(k)$ is not caused by a broadening of QP peaks but results from a strong temperature shift of ω_{QP} to positive values, $\omega > 0$.

Examining **k**-points far from the AF BZ edge, $k = (0,0), (0,\pi/2)$ we have found a more strong variation of QP peaks with T and δ (Fig. 1c,d, 2b). In this region of **k**-space the most pronounced effect of doping is an appearance of a band of incoherent states far below μ. These incoherent states manifest themselves as a smoothly **k**-dependent background in momentum distribution $N(k)$.

Therefore the main result of the present calculations is a weak concentration and temperature dependence of the spectral function (quasi-particle hole spectrum) while the momentum distribution function is proved to change dramatically with increasing temperature for $T > T_d$ with $T_d \simeq 1.5J\delta$.

In the present investigation we neglected any renormalization of the spin-wave excitation spectrum. Hence, an extension of the model (6) – (7) [5], [6] to the regime of moderate hole concentration $\delta \geq 10\%$, where one can expect a strong renormalization of the spin-wave excitations [8], seems to be questionable. But we can argue that due to a small radius of the AF polaron [7] and finite correlation length of AF fluctuations, even at higher doped cuprates [11], a qualitative description within the framework of the present model is possible.

A more reasonable self-consistent calculations allowing for the renormalization of AF spin-fluctuation spectrum will be considered in a separate publication.

Acknowledgments

One of the authors (N.P.) is greatly indebted to P.Fulde, K.Becker and P.Horsh for stimulating discussion.

Appendix: $T = 0$ limit

Here we consider a particular limit of zero temperature, $T = 0$, and show in this limit an equivalence of equations (17) and (22) – (26) with that derived within the standard diagrammatic technique in Refs. [5], [6], [8]. To this end it is convenient to change the notations as follows

$$\bar{G}(k,\omega) = G(k,\omega-\mu), \quad \bar{\Sigma}(k,\omega) = \Sigma(k,\omega-\mu) \qquad (A1)$$

Then the self-energy part $\Sigma_1(k,\omega-\mu)$, eq.(23), can be rewritten as

$$\bar{\Sigma}_1(k,\omega) = \sum_q M_1^2(k,q) \int_{-\infty}^{+\infty} d\varepsilon \frac{-1/\pi \mathrm{Im}\bar{G}(k-q,\varepsilon)}{\omega - \varepsilon - \omega_q + i\eta}[1 - n(\varepsilon-\mu) + N(\omega_q)]. \quad (A2)$$

By analogy with (A2) a similar formula for $\bar{\Sigma}_2(k,\omega)$ and the equation for the chemical potential $\mu = \mu(\delta,T)$ can be written straightforwardly from (24) and (26), respectively, with the replacement $n(\varepsilon) \to n(\varepsilon - \mu)$ in the integrands.

Let us consider now the case of a single hole, $\delta \to 0$, and $T = 0$. A value for the chemical potential $\mu_0 = \mu(0,0)$ in this case is determined by the equation

$$0 = \frac{1}{N}\sum_k \int_{-\infty}^{\mu_0} d\varepsilon(-\frac{1}{\pi})\mathrm{Im}\bar{G}(k,\omega), \qquad (A3)$$

from which one deduces that

$$\mathrm{Im}\bar{G}(k,\varepsilon) = 0, \quad \text{if} \quad \varepsilon < \mu_0, \qquad (A4)$$

and, hence,

$$\bar{\Sigma}_2(k,\omega) = 0. \qquad (A5)$$

Thus the value μ_0 defines a low energy cut off for the hole spectral density function that leads to

$$\bar{G}(k,\omega) = -\frac{1}{\pi}\int_{\mu_0}^{\infty} d\varepsilon \frac{\mathrm{Im}\bar{G}(k,\varepsilon)}{\omega - \varepsilon + i\eta} \qquad (A6)$$

The self-energy then takes the form

$$\bar{\Sigma}(k,\omega) = \bar{\Sigma}_1(k,\omega) = \sum_q M_1^2(k,\omega)\int_{\mu_0}^{\infty} d\varepsilon \frac{-1/\pi \mathrm{Im}\bar{G}(k-q,\varepsilon)}{\omega - \omega_q - \varepsilon + i\eta} =$$

$$= \sum_q M_1^2(k,q)\bar{G}(k-q,\omega-\omega_q). \qquad (A7)$$

Taking into account the Dyson's equation (17) which is written now as

$$\bar{G}(k,\omega) = [\omega - \bar{\Sigma}(k,\omega)]^{-1} \qquad (A8)$$

one comes to the equation for $\bar{\Sigma}(k,\omega)$ derived in Refs. [5], [6].

Examining in the same way a regime of finite doping $\delta \neq 0$ and $T = 0$, where, however, $\bar{\Sigma}_2(k,\omega) \neq 0$, we arrive at the equations of Ref. [8]. The only difference is that a retarded Green's function $\bar{G}(k,\omega)$, not causal one, is chosen in our calculations.

References

[1] J. Bonča, P. Prelovšek and I.Sega, Phys. Rev. B **39**, 7074 (1989); Y. Hasegava and D. Poilblanc, ibid. **40**, 9035 (1989); K.J. von Szczepanski, P. Horsch, W. Stephan and M. Ziegler, ibid. **41**, 2017 (1990); E. Dagotto, R. Joynt, A. Moreo, S. Bacci and E. Gagliano, ibid. **41**, 2585 (1990); ibid. **41**, 9049 (1990).

[2] S.A. Trugman, Phys. Rev. B **41**, 892 (1990); Phys. Rev. Lett. **65**, 500 (1990).

[3] R. Eder and K.W. Becker, Z. Phys. B **78**, 219 (1990); R. Eder, K.W. Becker and W.H. Stephan, ibid. **81**, 33 (1990); J.L. Richard and V.Yu. Yushankhai Phys. Rev. B **47**, 1103 (1993).

[4] S. Schmitt-Rink, C.M. Varma and A.E. Ruckenstein, Phys. Rev. Lett **60**, 2793 (1988).

[5] C.L. Kane, P.A. Lee and N. Read, Phys. Rev. B **39**, 6880 (1989).

[6] G. Martínez and P. Horsch, Phys. Rev. B **44**, 317 (1991).

[7] A. Ramšak and P. Horsch, Phys. Rev. **48**, 10559 (1993).

[8] J. Igarashi and P. Fulde, Phys. Rev. B **45**, 12357 (1992).

[9] N.M. Plakida, Phys. Lett. **A43**, 481 (1973); Yu.A. Tserkovnikov, Theor. i Matem. Fiz. **7**, 250 (1971); ibid. **49**, 219 (1981) (in Russian).

[10] M. Ziegler, Thesis, Karlsruhe University (1990).

[11] J. Rossat-Mignot et al., Physica C **185-189**, 86 (1991).

Received by Publishing Department
on March 1, 1994.